Development of a micro $CuInSe_2$ solar cell grown by electrodeposition

David Correia[1], Sascha Sadewasser[2], Pedro Salomé[2], Diana Leitão[1]

1. Instituto Superior Técnico (IST), Universidade de Lisboa, Av. Rovisco Pais, 1000-029 Lisbon, Portugal
2. International Iberian Nanotechnology Laboratory (INL), Av. Mestre José Veiga, 4715-330 Braga, Portugal

Abstract

This work concerns the electrodeposition of thin film $CuInSe_2$ absorber layers. An optimization of the electrodeposition geometry was carried out for deposition onto flat substrates consisting in a soda lime glass (SLG) coated with a molybdenum layer. A holder was built in order to get good reproducibility of the film growth. With the new holder several one step electrodeposition experiments were done varying the electrodeposition parameters such as deposition time, applied voltage, and solution concentration in order to find the best result and good quality $CuInSe_2$ thin films. Electrodepositions with solutions not containing Se were also done, however, with limited success. The samples fabricated by electrodeposition were treated by annealing using two different approaches: a closed atmosphere rich in Se and an open atmosphere with Se were a flow of N_2 was passing above the sample. After optimization was done for both processes, electrodeposition and annealing, the best recipes were applied to micropatterned substrates to be used in a concept of micro concentrator solar cells.

The samples produced were extensively characterized by scanning electron microscopy, energy dispersive X-ray spectroscopy, X-ray diffraction, Raman spectroscopy and stylus profilometry.

Key words: Electrodeposition, $CuInSe_2$, Solar Cell, Micro Concentrator

1. Introduction

Most of the present global energy production is accomplished by burning fossil fuels, therefore in the last years there has been an increase in the search for solutions in alternative sources of energy in order to suppress the dependence in limited resources and technologies that are potentially harmful to the environment. The source of energy that presents the biggest potential is the sun.

Photovoltaics is the area of knowledge that studies the conversion of sun radiation in direct current electricity using materials that exhibit the photovoltaic effect. The name comes from the conversion of light (photons) into electric power (voltage) (1).

Sunlight is available in most locations, and it provides such an enormous supply of renewable energy that if the whole global electricity demand would be covered exclusively by photovoltaics, the total land area needed for light collection would be only a few percent of the world's desert area (2).

The photovoltaic effect was first observed in 1839 by Edmond Becquerel, but the first patent for a 'solar cell' was received by Edward Weston only in 1888. The commercial stage of photovoltaics only began in 1954. Bell Laboratories while working on silicon semiconductors discovered that silicon had photoelectric properties and built the first photovoltaic module with around 6% efficiency. The first massive use of PV systems began in the 1960s to power space satellites. Throughout the years the technology advanced, reliability improved and the production costs began to decline. During the energy crisis in the 1970s, photovoltaic technology gained recognition as a source of power for non-space applications.

One of the main obstacles for photovoltaics to become more popular in the short term is the fact that the price of the electricity (cost per watt-hour) produced by photovoltaics is in most cases not yet competitive with that produced by conventional methods. Cost reduction can be achieved by either improving the values of efficiency or by reducing the production costs of photovoltaic modules. The production costs is expected to go down with increasing production volumes, due to market scale effects, and the efficiency has been highly improving along the years (3).

2. Thin-film solar cells

Thin-film solar cells have several advantages compared with crystalline Si solar cells. They are based in semiconductors with direct bandgaps which provide them with high absorption coefficients and therefore can be used in thin film form (4). Consequently, the material consumption is highly reduced due to layers only a few micrometers thick. Thin films can be deposited by a variety of vacuum and non-vacuum methods on inexpensive substrates such as glass. Another advantage is the possibility of using flexible substrates leading to lighter modules and creating novel opportunities for small harvesting devices.

The main candidates for low-cost thin film solar cell materials are amorphous hydrogenated silicon (a-Si:H), CdTe (cadmium telluride), and $CuInSe_2$ based compounds.

2.1 Structure

The structure of a thin film solar cell consists in a back contact, a p-type semiconductor, a n-type

buffer layer, and a top contact. In a typical $CuInSe_2$ (CIS) solar cell a molybdenum layer is used as back contact, an undoped ZnO, and doped ZnO:Al layer as top contact. CdS is usually used as buffer layer, see Fig. 2.1.

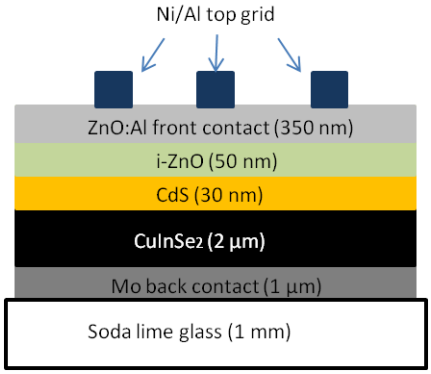

Fig. 2.1- Structure of a $CuInSe_2$ solar cell with typical thickness values for each layer.

This type of structure is complex because it is a stack of several layers that may react with each other, however these detrimental interface reactions are inhibited at ambient temperatures.

2.2 Micro concentrator concept

$Cu(In,Ga)Se_2$ thin film solar cells are based in elements that are not abundant on earth, like Ga and In, and, therefore, expensive (5). The scarcity of these elements requires a reduction of the used material in order to enable material savings that allow for cheaper solar cells (6) (7). The micro concentrator concept is based on using micrometer-sized patterned solar cells onto which sunlight is concentrated using a lens array, see Fig. 2.2. A concentrator device requires the surface to be only partially covered by solar cells which creates significant material savings (8).

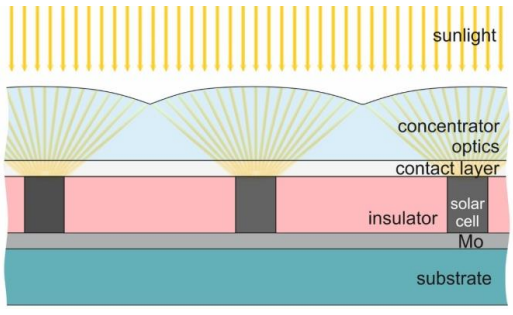

*Fig. 2.2- Concept of the micro-concentrator solar cell **(9)***

The samples used in this work were produced with clean room technology followed by electrodeposition of $CuInSe_2$ and thermal annealing treatment, Fig. 2.3. A SiO_2 layer (2µm) was deposited by chemical vapor deposition (CVD) on top of a soda lime glass (SLG) coated with a Molybdenum layer (1µm) and using lithography, a pattern is written in the SiO_2 and etched with reactive ion etching (RIE).

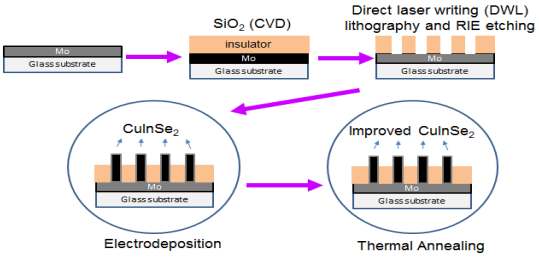

Fig. 2.3- Schematic of sample growth procedure.

3. Experimental Techniques

3.1 Electrodeposition

Electrodeposition is a chemical method to grow good quality films at low temperatures and low production cost. The process is based on moving ions through a solution by applying an electric filed in order to coat an electrode (working electrode). The system consists on a 3-electrode cell powered by a potentiostat. The 3-electrode cell is composed by: working electrode, counter electrode and reference electrode. The working electrode is where the electrodeposition occurs and in this work the substrate used was soda lime glass (SLG) coated with a 1µm thickness molybdenum layer (substrates are 2.5 cm x 2.5cm). The counter electrode supplies current to the reaction on the working electrode and in this work a platinum mesh made with a 0.2 mm diameter platinum wire was used as counter electrode. The reference electrode electrode should have a stable reference potential and its task is to measure the voltage on the working electrode versus its own, in this work a satured calomel electrode (SCE) was used.

All the experiments in this work were done with potensiostat in chronoamperometry mode, which means the voltage was defined and the current was free to oscillate during the experiment. It is important to fix the voltage since the growth of CISe ternary compound is very sensitive (10), see (Fig. 3.1). The current that passed through the sample was defined by the number of ions present in the solution and by the area of the sample, the bigger the sample and the amount of ions present in the solution the bigger will be the flux and therefore bigger current values. By knowing the current density value during the experiment and the area of sample it is possible to estimate the thickness of the film we are depositing and the time needed to obtain the desired thickness.

The solution stoichiometry and the applied voltage were based on (11), and it was not varied since the $CuInSe_2$ electrodeposition growth

procedure is very sensitive as can be shown in Fig. 3.1.

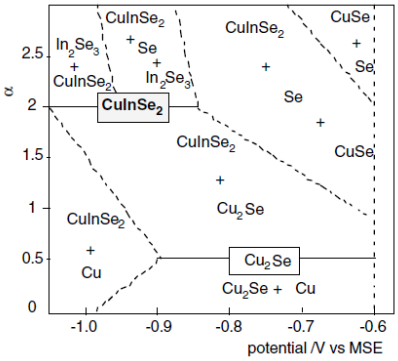

Fig. 3.1- Electrochemical phase diagram showing the effect of one step electrodeposition parameters in the composition of CIS. films. The composition of the films is showed as a function of the electrodeposition potential and the flux ratio between selenium(IV) and copper(II) ionic species. The indium concentration is assumed to be in excess. The potential is given with respect to a Sulfate Mercurous Electrode (MSE, 0.40V vs SCE) ***(12)****.*

3.2 Annealing

Growing by electrodeposition does not provide thin films with a good electronic quality, because it is a low temperature process and the material grows amorphous and/or with poor crystalline quality. Therefore, samples need to go through thermal annealing treatments to improve the structural, electronic, and optical properties of the film. Thermal annealing can be done under vacuum or atmospheres with a desired composition (13).

For CISe films annealing treatments are generally carried out for temperatures ranging from 450ºC to 650ºC from a few minutes to one hour or more (12). At these temperatures $CuInSe_2$ is not stable and Se evaporates from its surface, therefore the annealing needs to occur under a rich selenium atmosphere in order to keep a high selenium pressure on the sample to not lose the selenium already deposited during electrodeposition (14). In this work a setup with a closed atmosphere (Fig. 3.2) was tested:

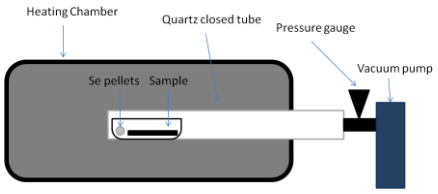

Fig. 3.2- Diagram for closed atmosphere used in thermal annealing

The sample is placed, together with selenium pellets, inside a graphite box that slides in the quartz tube to be placed in the center of the heating chamber. The tube is filled with N_2 to a previously defined pressure in the beginning of the experiment and there is no flow during the experiment.

4. Results

4.1 Electrodeposition geometries

There are different possibilities to perform electrodeposition. The geometry used for the electrodeposition has a great influence in the deposited thin films. Since potentiostatic electrodeposition uses several intervenients such as three electrodes and a magnet there is a range of geometries that can be studied to determine the most suitable.

To find the geometry that provides more homogeneity to the films two setups were tested: i) a vertical setup, were the sample surface is in the vertical position (Fig. 4.1 a)) and ii) a horizontal setup, were the sample surface is in the horizontal direction (Fig. 4.1 b)).

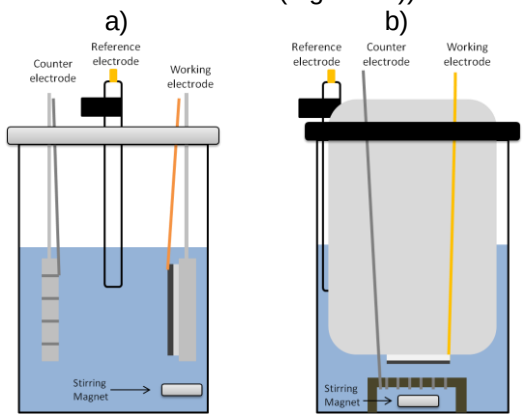

Fig. 4.1- a) Sketch of vertical setup and b) Sketch of horizontal setup.

In the first experiments the solution used was (solution 2 in Table 4.2):

- **$In_2(SO_4)_3 \cdot 6H_2O$:** 332 mg,
- **SeO_2:** 71 mg,
- **$Cu_2SO_4 \cdot 5H_20$:** 38 mg,
- **$LiSO_4$:** 5.3 g,
- **H_20:** 100 ml.

For both geometries a stirring velocity of 60rpm and a deposition voltage of -0.55V were used. For each setup a sample was produced and was analyzed by SEM, the results are found in Fig. 4.2. From these images we clearly see a higher homogeneity in the film deposited with the vertical geometry. The sample deposited with the horizontal set up shows a significant number of voids where there was no deposition or the deposited film is too thin. The voids were caused probably by bubbles developing on the substrate during the deposition.

a) b)

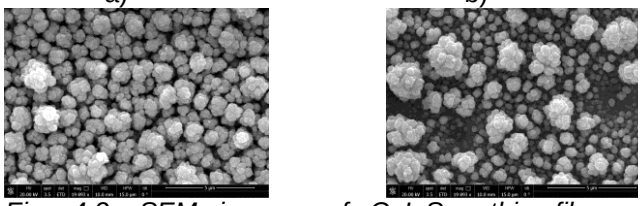

Fig. 4.2- SEM images of $CuInSe_2$ thin films deposited from solution 1 with -0.55V and 60rpm. a) using a vertical geometry and b) using a horizontal geometry. Both images were taken with a beam acceleration voltage of 20 kV and a (Horizontal Field Width) HFW of 15 µm.

From this experiment we see that the higher concentration slightly made deposition from horizontal geometry more homogeneous than in the last experiment, however vertical geometry still gave the best result in terms of morphology.

Based on the visual analysis of samples, the smooth film morphology and the better homogeneity we selected the vertical setup for the rest of the thesis work. To have better reproducibility a holder was built. It consisted in three pieces made of Teflon: a round piece where the electrodes where held, a piece where the platinum wire was wrapped around to make the mesh, and a third piece where the sample was placed, see Fig. 4.3.

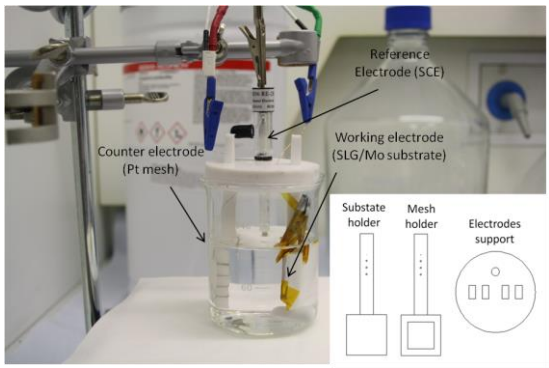

Fig. 4.3- Picture of the electrodeposition setup and schematic of the three pieces built for the electrodeposition sample holder (inset).

For the vertical setup further tests were performed where several parameters of the geometry were varied to see the influence in the growth of the films and to find the best geometry. The parameters varied were the distance between working and counter electrode, magnet position and sample orientation. The combination of the values tested for those parameters are given in Table 4.1:

Table 4.1- Different geometries used for vertical electrodeposition

Geometry	Distance between electrodes (cm)	Magnet position	Sample orientation
1	3	Under sample	Facing the CE
2	3	Under sample	Facing the glass
3	1	Under sample	Facing the CE
4	3	Under CE	Facing the CE

Pictures of the samples after electrodeposition were taken in order to visually compare the differences, see Fig. 4.4. At first sight it is clear that placing the sample facing the glass (geometry 2) is not a good option since the film is very inhomogeneous and has a bright color, characteristic of the molybdenum layer, near the edges which indicates that the film is very thin. The other three samples are more similar, however it is possible to see that the last sample (geometry 4) has some color changes along the surface, indicating a larger roughness. Between samples electrodeposited with geometry 1 and 3 it is not possible to conclude anything visually, however both of them look good.

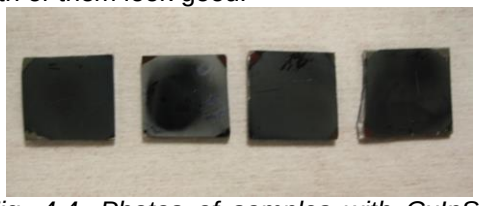

Fig. 4.4- Photos of samples with CuInSe2 thin-films electrodeposited vertically using geometry 1, 2,3, and 4 from left to right.

To have a more detailed analysis of the effect of the geometries on the thin film growth SEM characterization was performed, see Fig. 4.5. With SEM images it became clear that the best geometries were 1 and 3, which revealed the most homogeneous morphology and topography. In sample 2 (dark area) and 4 there are very different grain sizes causing the roughness that was possible to see visually. Comparing again geometries 2 and 4 it is possible to say that the sample grown with geometry 1 is the most homogenous since in sample from geometry 3 it is possible to see some larger grains that are not seen in first sample.

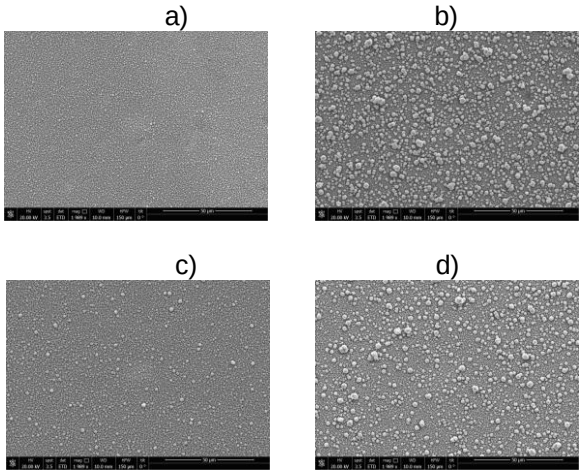

Fig. 4.5- SEM images of samples with $CuInSe_2$ thin films electrodeposited vertically using geometry a) 1, b) 2, c) 3, and d) 4. All images were taken with a beam voltage of 20kV and a HFW of 150µm.

This set of experiments reveal the best geometries to be 1 and 3, the difference between the two is the electrodes distance. The geometries where the orientation of the sample (2) and the position of the magnet (4) were changed lead to samples with big inhomogeneities and clear differences in the grain sizes. These geometries produced inhomogeneities at a large scale, as seen in the optical images, as well as in a small scale, as seen in the SEM images. The parameter with less influence in the geometry was the distance between electrodes, however the thin film electrodeposited with the electrodes farther from each other is the one with the most homogeneous topography. Therefore geometry 1 was selected for the rest of the work.

4.2 One step electrodeposition

In this chapter $CuInSe_2$ thin films that were formed by single electrodeposition process and where the solution contained all three elements (Cu, In, and Se) in the bath will be presented. Several conditions were tested, including: the stirring velocity (section 4.2.1), concentration of solution (section 4.2.2), duration of electrodeposition and reproducibility (section 4.2.3).

4.2.1 Influence of the stirring velocity

The first parameter to be tested was the stirring velocity, using the following solution (solution 1):

- **$In_2(SO_4)_3 \cdot 6H_2O$:** 1658mg,
- **SeO_2:** 353mg,
- **$Cu2SO4 \cdot 5H_20$:** 191mg,
- **$LiSO_4$:** 5.3g,
- **H_20:** 100ml.

Three samples were grown with three different stirring velocities: 60, 400, and 1000 rotations per minute (RPM). SEM images of the grown films can be seen in Fig. 4.6.

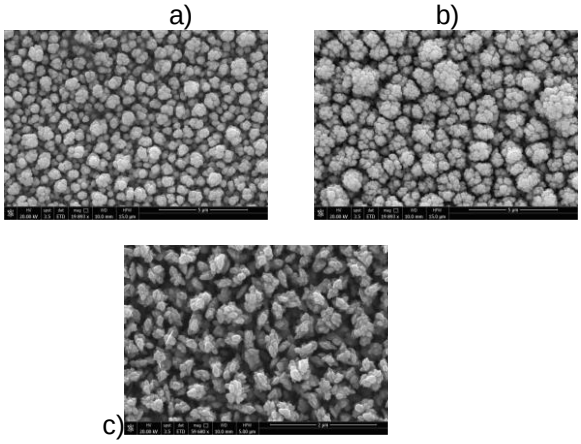

Fig. 4.6- SEM images of $CuInSe_2$ thin films deposited from solution 2 with -0.55V and a) 60rpm, b) 400rpm, and c) 1000rpm. All images were taken with a beam voltage of 20kV and a HFW of 15µm.

These experiments show that stirring has a big influence on the morphology and also on the structure. For lower stirring velocities the structures have a round form, a cauliflower-like structure and for higher velocities (1000rpm) the structure grows more in a longitudinal way. The velocity that grew the bigger grains and the most compact film was 400rpm.

4.2.2 Influence of the solution concentration

Another study that was made was the influence of the solution concentration in the thin film growth. Different concentrations were tested to see the effect on the thin film morphology. Table 4.2 shows the different solutions used.

Table 4.2- Different solutions used along experimental tests.

	Solutions used				
	$In_2(SO_4)_3 \cdot 6H_2O$ [mg]	**SeO_2 [mg]**	**$CuSO_4 \cdot 5H_2O$ [mg]**	**H_20 [ml]**	**$LiSO_4$ [g]**
Solution 1	1658	353	191	100	5.3
Solution 2	332	71	38	100	5.3
Solution 3	111	24	13	100	5.3

Three samples were grown by electrodeposition using a different solution for each one and using an applied voltage of -0.55 V and 400 rpm stirring velocity. The results of the SEM characterization are shown in Fig. 4.7.

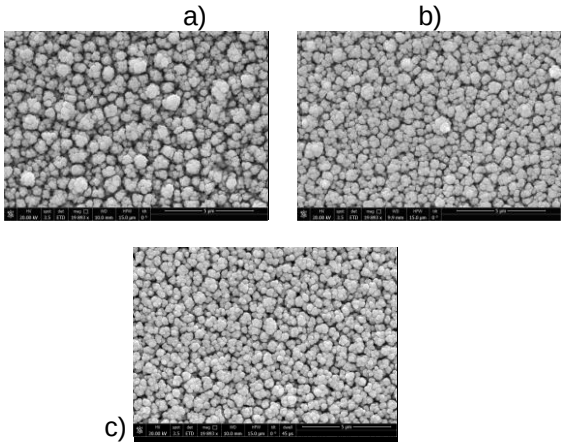

Fig. 4.7- SEM images of $CuInSe_2$ thin films deposited from a) solution 1 (Sample A), b) solution 2 (Sample B), c) solution 3 (Sample C) with -0.55 V and 400 rpm. All images were taken with a beam voltage of 20kV and a HFW of 15µm.

Images show that for the higher concentration solution (solution 1, sample A) the film is less compact than for the other solutions. Samples from solution 2 and 3 look very similar and there is no evidence of any significant difference between them.

Some further characterization was done both for thickness and chemical composition, Table 4.3. In terms of composition we see similar values for samples B (solution 2) and C (solution 3) both for [Cu]/[In] and [Se]/[(Cu+In)] ratios, however sample A (solution 1) has a very different [Cu]/[In] ratio than the other samples. Again sample B and C are the most similar.

Table 4.3- Deposition parameters and characterization made on samples.

	I (mA)	Time (s)	Thickness (µm)	[Cu]/[In]	[Se]/[(Cu+In)]
CISe 160310-A	-56	300	1.80	1.44	1.42
CISe 160315-A	-10	1700	1.53	0.89	1.35
CISe 160322-A	-3	7600	1.91	0.83	1.34

It Is apparent that for the most concentrated solution the current value is higher, which is expected since there are more ions in the solution. In order to get the same thickness the electrodeposition time was changed to have the same amount of ions in the film (the value of Current*Time was kept constant).

In this section some optimization of electrodeposition parameters was done. The experiments with the stirring velocity revealed the best results for an intermediate stirring velocity (400rpm). The influence of concentration of solutions in the growth was also studied and it was found that is best to use less concentrated solutions if we want to get a more homogeneous and compact film. However for higher concentrations the deposition is much faster than with lower concentrations what may be important in a commercial scale.

4.3 Thermal Annealing

Growing by electrodeposition do not provide thin films with a good electronic quality, because it is a low temperature process and the material grow amorphous and/or with poor crystalline quality. Therefore samples need to go through thermal annealing treatments to improve the structural, electronic, and optical properties of the film.

Like in the electrodeposition case we had different possibilities for the experimental setup and some tests had to be done to choose the best option: open or closed atmosphere and sample positioning/settling inside furnace. Beside the experimental setup other parameters can be controlled such as time, temperature, pressure, and selenium present in the atmosphere.

A set of experiments was done varying the annealing time and temperature. SEM images are shown in Fig. 4.8.

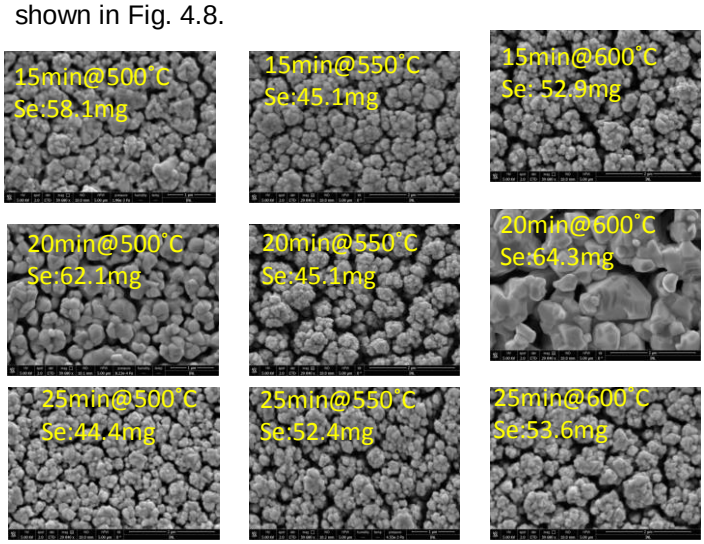

Fig. 4.8- SEM images of annealed samples with different annealing time, temperature and Se used. The images were taken with an electron beam voltage of 5kV and a HFW of 5µm.

From the sample morphology it is not possible to find any trend along the annealing time or temperature. This may be related with the amount of selenium used in the processes. The selenium was used in small pellets and the weighing was a discreet process what caused some difficulties in obtaining from run to run the

same amount of selenium. However, the sample that looks more crystalline is the one annealed at 600˚C during 20 minutes and this was the recipe used in the next steps. It cannot be ruled out that this sample is an outlier since it is quite different from all other ones. Also the non-reproducibility of the process can be an issue, since the mounting and positioning of the sample is done manually and there might be unknown changes crucial to the process which are not reproduced. The composition ratios are with agreement with SEM images. the best ratios are found to be the ones from sample annealed at 600ºC during 20 minutes ([Cu]/[In] = 0.83 and [Se]/[Cu+In] = 0.96). On the other side the worst ratios ([Cu]/[In] = 0.70 and [Se]/[Cu+In] = 1.31) are the ones from the sample that looks less crystalline. sample annealed at 550ºC during 20 minutes. XRD characterization was carried out for all samples and comparison by annealing temperature was done, see Fig. 4.9. The characteristic peaks from tetragonal $CuInSe_2$ are present in all samples and no other phases of CISe coumpounds are seen, which indicates that the stoichiometry during electrodeposition and the annealing temperature range are within acceptable values to form $CuInSe_2$. Naturally significant peaks from the bottom layers are also found in XRD spectrum such as SiO_2 and Mo.

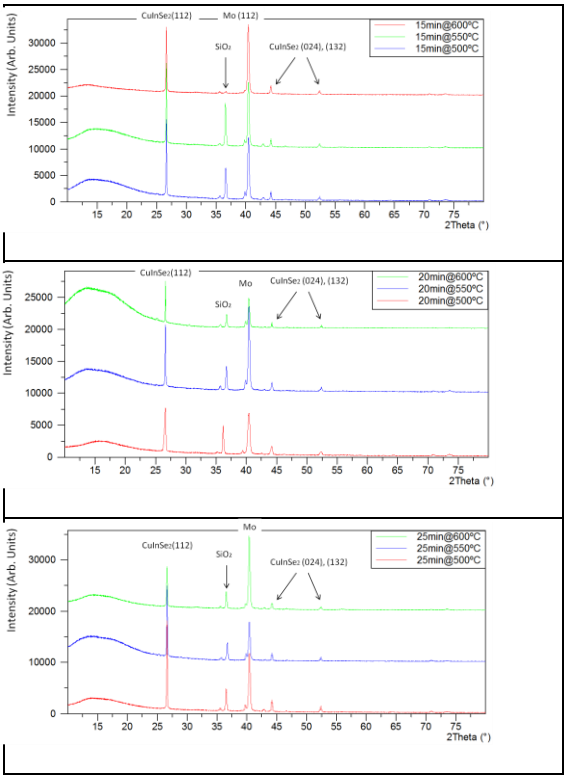

Fig. 4.9- XRD spectrums of annealed samples at different temperatures (500ºC, 550ºC and 600ºC) and with different times (15 min, 20 min and 25 min).

4.3.1 Selenium Study

An experiment was carried out to verify the hypothesis of strong dependence of the annealing with the selenium present in the atmosphere; three samples from the same precursor were annealed (600˚C during 20 minutes) in atmosphere with different selenium amounts, SEM images can be seen in Fig. 4.10.

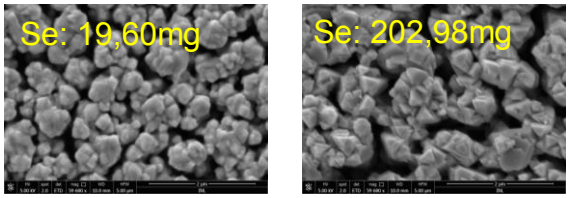

Fig. 4.10- SEM images of annealed samples in different selenium atmospheres.

The SEM images show a clear difference between samples. A higher crystallinity is present when more selenium was used. The increased crystallinity suggests that annealing must occur in an excess selenium atmosphere and it is in accordance with the literature (14). Also the composition ratios, shown in Table 4.4, are closer to the desired ones for the sample in the richest selenium atmosphere.

Table 4.4- List of samples used in the selenium study with selenium used and composition ratio before and after annealing.

Sample	Se (mg)	[Cu/In]	[Se]/[(Cu+In)]
Precursor	-	0.93	1.27
CISe160318C-P1	19.60	0.80	1.16
CISe160318C-P3	202.98	0.83	1.01

4.4 Micropatterned $CuInSe_2$

In this chapter I will first present the electrodeposition on the micro-patterned substrates. Secondly, the thermal annealing results of the micro-patterned substrates to be used in the concept of a micro-concentrator solar cell will be presented.

4.4.1 Electrodeposition

Since electrodeposition needs an electrical conductor to work and this substrates only have electrical conductivity where they are covered with Mo it is possible to have selective electrodeposition. In this way, as desired, there will

be only deposition in the holes and no deposition on the SiO_2 area.

The obvious approach was to use the best result obtained in the flat substrates. The first test was done using solution 2 with an applied voltage of -0.55 V, a stirring velocity of 400 rpm, and a deposition time of 2000 s. SEM images with different amplifications and of different areas of this sample are shown in Fig. 4.11.

a) b)

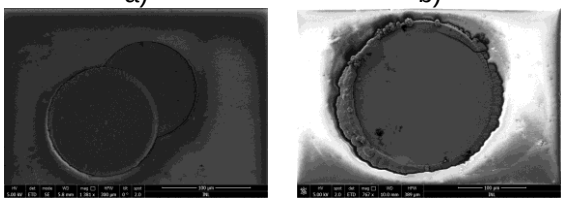

Fig. 4.11- SEM images of the micro-patterned CISe. All images were taken with a beam voltage of 5kV. a) CISe that moved from where it was deposited to the top of other structure during electrodeposition b) Structure overfilled with CISe.

This experiment revealed two different problems. Overgrowth of CISe around the structures (Fig. 4.11 b)) and movement of material after it was electrodeposited in the patterns (Fig. 4.11 a)). To avoid the overgrowth, the deposition time had to be decreased in order for the films not to grow over the structures. The movement problem was probably due to the high stirring velocity.

The first hypothesis to test was to decrease the stirring velocity keeping the solution the same and sample H-CIS160629-A was grown with conditions shown in Table 4.5.

Table 4.5- Deposition parameters to study overgrowth and movement during growth.

	Deposition parameters			
Sample	**V (V)**	**Stirring (rpm)**	**I(mA)**	**Time (s)**
H-CIS160629-A	-0.55	60	-1.8	2000

To investigate if the movement of material was avoided during the deposition SEM characterization was carried out, see Fig. 4.12.

a) b)

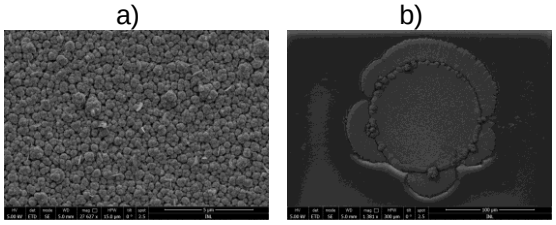

c)

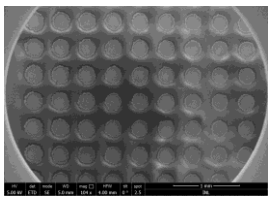

Fig. 4.12- SEM images of the micro-patterned CISe (H-CIS160629-A). All images were taken with a beam voltage of 5kV. a) Image of the film inside the structure. b) Structure overfilled with CISe. c) Pattern entirely filled with electrodeposited CISe.

In this experiment there are no more evidences of the material moving. Thus, we conclude that for the previous experiment, the deposited $CuInSe_2$ was being removed from its original position due to the high stirring speed. The next step was to avoid the overgrowth around the structures. The hypothesis of decreasing the time, and consequently the amount of material deposited, was tested and a new sample was grown with deposition parameters shown in Table 4.6.

Table 4.6- Deposition parameters to study overgrowth and movement during growth.

	Deposition parameters			
Sample	**V (V)**	**Stirring (rpm)**	**I(mA)**	**Time (s)**
H-CIS160718-A	-0.55	60	-1.3	900

To investigate if the overgrowth problem was overcome SEM characterization was carried out, see Fig. 4.13.

a) b)

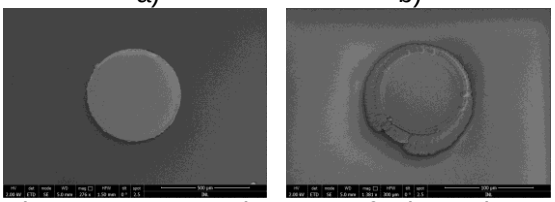

Fig. 4.13- SEM images of the micro-patterned CISe (H-CIS160718-A). All images were taken with a beam voltage of 5kV. a) 500µm diameter structure correctly filled with electrodeposited CISe b) 80µm diameter structure overfilled with electrodeposited CISe.

The overgrowth was avoided for the bigger structures but not for the smaller ones (Fig. 4.13).This fact indicates a variation of the deposition rate with the hole diameter. The thickness values were measured using a thickness profiler for 7 holes. With the characterization along the holes became clear that there is a dependence

of the deposition thickness with the hole diameter, for bigger holes the deposited film is thinner than for bigger holes. Also, the overgrowth of film around the hole starts when the film thickness is around 2 µm, which is the hole depth. The electrodeposition time also has an important role in the thickness of the electrodeposited material therefore the electrodeposition time in structures with different sizes was investigated and a comparison between samples grown in same conditions but with different deposition times was made, Fig. 4.14.

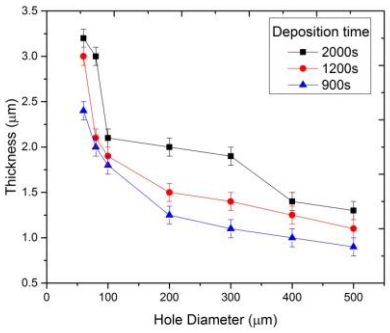

Fig. 4.14- Evolution of thickness of electrodeposited CISe according to structure diameter and deposition time. All samples were deposited in the same conditions where only the total time was varied.

Fig. 4.14 confirms a strong dependence of electrodeposited thin-film thickness both on hole diameter and deposition time. It can also work as a calibration curve to choose the deposition time if we have a substrate with a well-defined pattern containing the same depth and diameter structures.

4.4.2 Annealing

The best results in annealing of the flat surface samples were applied to the micro patterned samples. The annealing time used was kept constant at 20 minutes. However some different behaviour was found when moving from flat surfaces to micro patterned surfaces, some annealing parameters had to be tuned in order to meet the differences in the behaviour of this samples during the annealing. The first encountered problem found was the peel off of SiO_2 layer around the holes in sample H-CIS160623 (Fig. 4.15).

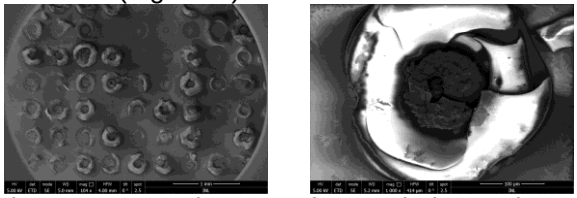

Fig. 4.15- SEM images of annealed sample H-CIS160623. Images were taken with an electron beam voltage of 5kV.

This problem might be related with the formation of a $MoSe_2$ layer. At elevated temperatures Se diffuses trough the CISe layer and reaches the Mo to form $MoSe_2$ (15). When passing from Mo to $MoSe_2$ the material expands and this might lead to the peeling off of the SiO_2 close to the holes. Thus. the high temperature. 600ºC. revealed to be too much for the SiO_2 layer. The next step was to decrease the temperature of the annealing to 500ºC as it was done for H-CIS160629-A (Fig. 4.16).

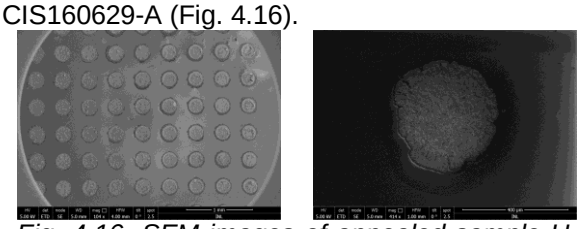

Fig. 4.16- SEM images of annealed sample H-CIS160629-A. Images were taken with an electron beam voltage of 5kV.

The problems with the SiO_2 layer were avoided by decreasing the annealing temperature. EDS characterization (Fig. 4.17) and Raman spectroscopy (Fig. 4.18) were carried out micro-CISe islands with different sizes to study the composition and crystal quality of the CISe material:

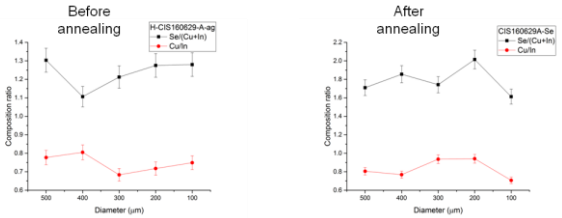

Fig. 4.17- Composition ratios of as grown sample (H-CIS160629-A-ag) and after annealing (H-CIS160629-A-Se) for different hole sizes.

EDS characterization data (Fig. 4.17), show, despite some fluctuation, nearly constant composition ratios along the different holes before and after annealing. The [Cu]/[In] ratio (red line) is roughly around 0.8 before and after annealing however the annealing turned the sample slightly copper richer. In [Se]/([Cu]+[In]) (black line) we see that there is a big difference between both samples, before annealing the ratio is around 1.2 and after annealing it changed to 1.8. The annealing highly increased the selenium present in the sample.

Fig. 4.18 shows a Raman analysis before and after the annealing. Before the annealing, red curve, the plot shows a broad peak centered at 174 cm^{-1} which corresponds to the characteristic A1 vibration of the $CuInSe_2$ structure. After the annealing, the signal to noise ratio vastly improves as well as the intensity of the signal, showing a clear improvement in the crystal quality of the sample. Now both peaks, A1 at 174 cm^{-1} and B1 at

220 cm^{-1} are well defined, clearly showing that the $CuInSe_2$ tetragonal structure is present with good crystalline quality.

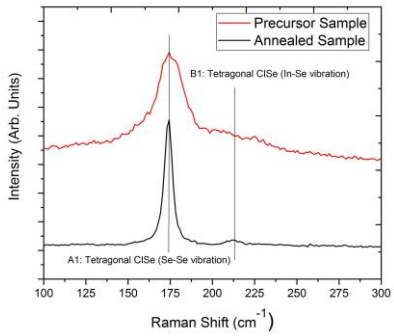

Fig. 4.18- Comparison between Raman spectrum of sample H-CIS-160629-A before (ag) and after annealing (Se).

A Raman analysis was performed in sample H-CIS-160629-A-Se where a big number of holes was measured, see Fig. 4.19. It was noticed that all of the holes had the main vibration of the CISe structure. However, it should be noted that there was a big difference in quality among the holes. For instance, in the two biggest holes (500 µm and 400 µm) the crystal quality appears to be quite high as shown by the appearance of an extra peak, this peak is often seen in selenium rich films (16). The smallest hole showed the worst crystal quality since the main CISe vibration is very broad and with low intensity. These results should be taken carefully since only a few holes were analyzed. There are hundreds of structures and a careful analysis of all of the holes or one with significant statistical analysis was not performed in this thesis due to lack of time.

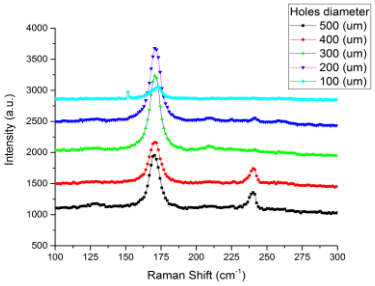

Fig. 4.19- Raman spectrum of different sized holes in sample H-CIS-160629-A-Se.

5. Conclusions

In the electrodeposition geometry optimization it was found that the vertical setup grew very homogeneous samples while thin films grown with the horizontal setup had voids in the surface. In the tuning of parameters of vertical setup it was clearly seen that the sample surface needs to be facing the counter electrode to get nice deposition and the best result was found for a sample grown while the stirring magnet was under the sample and when the working electrode and counter electrode were more distant (3 cm).

The single step electrodeposition experiments with the stirring velocity revealed the best results for an intermediate stirring velocity (400 rpm). The influence of concentration of solutions in the growth was also studied and it was found that is best to use less concentrated solutions if we want to get a more homogeneous and compact film. However for higher concentrations the deposition is much faster than with lower concentrations what may be important in a commercial scale.

Annealing treatments were carried out using two different approaches, a closed atmosphere and an open atmosphere both rich in selenium. The open atmosphere setup was a failed approach since the samples were losing the selenium already present from the electrodeposition. The closed atmosphere setup showed the best results, producing samples with composition ratios near the optimal values. XRD showed that the structure present in the film was a tetragonal $CuInSe_2$. Experiments with different selenium concentrations in the atmosphere revealed that excess selenium in the atmosphere is important to get a better crystallinity.

After optimization of the electrodeposition and annealings these two processes were used in the micro patterned substrates and some difficulties were found. First, during electrodeposition It was seen that the electrodeposited material moved out from the holes due to the high stirring velocity (400 rpm) and it needed to be decreased, 60 rpm was used. The thickness of the electrodeposition was found to be a function of not only the electrodeposition time but also the hole diameter. In the annealing of this samples it was found that the optimal temperature for flat surfaces, 600ºC, was too high, leading the SiO_2 close to the holes to peel off. However good results were obtained with lower annealing temperatures as it was verified by Raman spectroscopy the crystallinity improvement after annealing.

6. Future Studies

The next steps are to conclude the full solar cell and perform tests to verify the concept of micro concentrator solar cell. A good way of depositing CdS on top of the micro patterned substrate filled with electrodeposited CISe maybe chemical bath deposition (CBD), which is already being developed in INL by LaNaSC group. Some experiments in depositing the ZnO:Al layer with atomic layer deposition (ALD) are also being done. Also some considerations for inkjet printing of the

top grid are being studied. However these processes need to be optimized. Another fundamental thing that needs to be built is a set of lens on top of the cell to concentrate the light on the holes covered with $CuInSe_2$.

After building the full micro concentrator solar cell, several characterization tests can be done to get the relevant parameters in a solar cell, such as efficiency and field factor, and verify the utility, consistency and effectiveness of the concept.

7. References

1. *Photovoltaic materials, history, status and outlook.* **A. Goetzberger, C. Hebling and H. W. Schock.** s.l. : Materials Science and Engineering, 2003.
2. *Solar Cells and their Applications.* **Partain, L. Fraas and L.** s.l. : John Wiley & sons, INC, 2010.
3. *Solar cells: past, present, future.* **A. Goetzberger, J. Luther and G. Willeke.** s.l. : Solar Energy Materials and Solar Cells, 2002.
4. *Recent developments in photovoltaics.* **Green, M. A.** s.l. : Solar Energy, 2004.
5. *Materials availability expands the opportunity for large-scale photovoltaics deployment.* **C. Wadia, A. P. Alivisatos and D. M. Kammen.** s.l. : Environmental Science & Technology, 2009.
6. *Thin-film microcells: a new generation of photovoltaic devices.* **al, M. Paire et.** s.l. : SPIE Newsroom, 2013.
7. *Cu(In,Ga)Se2 microcells: high efficiency and low material consumption.* **al, M. Paire et.** s.l. : Journal of Renewable and Sustainable Energy, 2013.
8. *Microscale solar cells for high concentration on polycrystalline Cu(In,Ga)Se2 thin films.* **al, M. Paire et.** s.l. : Applied Physics letters, 2011.
9. **Sascha Sadewasser, Pedro Salomé, Humerto Rodriguez Alvarez.** submitted (2016), Solar Energy Materials and Solar Cells.
10. *Ternary and Multinary Compounds .* **R. D. Tomlinson, A. E. Hill and R. D. Pilkington.** s.l. : Proceedings of the 11 th International Conference on Ternary and Multinary Compounds, 1997.
11. *Electrodeposition od CuInSe2 absorber layers from pH buffered and non buffered sulfate-based solutions.* **C. Sene, M. E. Calixto, K. D. Dobson and R. W. Birkmire.** s.l. : Science Direct, 2007.
12. *Chalcopyrite thin film solar cells by electrodeposition.* **al, D. Lincot et.** s.l. : Science Direct, 2004.
13. *Effect of bath temperature and annealing on the formation of CuInSe2.* **M. Benaicha, N. Benouattas, C. Benazzouz, L. Ouahab.** s.l. : Solar Energy Materials and Solar Cells, 2009.
14. *One step electrodeposition of CuInSe2: improved structural, electronic, and photovoltaic properties by annealing under high selenium pressure.* **al, J. F. Guillemoles et.** s.l. : Journal of Applied Physics, 1996.
15. *CuInSe2 precursor films electro-deposited directly onto MoSe2.* **al, C. Y. Cummings et.** s.l. : Journal of Electroanalytical Chemistry, 2010.
16. *Composition dependence of the Raman A1 mode and additional mode in tetragonal Cu–In–Se thin films.* **al, Chuan-Ming Xu et.** s.l. : Semiconductor Science and Technology, 2004.